A shape-adaptable organometallic supramolecular coordination cage for the encapsulation of fullerenes

Víctor Martínez-Agramunt,[a] Dmitry G. Gusev[b] and Eduardo Peris*[a]

**Abstract:** The development of three dimensional supramolecular coordination complexes (SCCs) with cavities suitable for guest binding is of great interest because these materials are useful in a large number of applications. Herein, we describe a nickel-conjoined organometallic molecular prism, which has been fully characterized. The X-ray diffraction structure of the molecule reveals that the cage possesses an internal cavity with a volume of 1028 $Å^3$, thus suitable for the encapsulation of large 3D-molecules, such as fullerenes. This cage shows highly selective complexation of C_{70} over C_{60}, thus being potentially useful for fullerene separation and purification. The combined experimental and computational studies suggest that the complexation process is largely entropically-driven, and that the cage is flexible and can adapt the size and the shape of the cavity to maximize the face-to-face interaction with the fullerenes.

Introduction

The rich coordination chemistry of transition metals and the availability of a large number of organic ligands have provided access to many two- and three-dimensional metallosupramolecular architectures with applications in catalysis,[1] molecular recognition,[2] for stabilizing highly reactive species,[3] and as drug delivery/release vectors.[4] Of particular interest are supramolecular coordination complexes (SCCs) with well-defined cavities suitable for guest binding[5]; the host-guest chemistry arguably being the most important feature of SCCs, from which most applications can be derived. In particular, the selective encapsulation of large aromatic compounds, such as fullerenes[6] and polycyclic aromatic hydrocarbons (PAHs)[7] is of increasing interest since it may provide practical solutions for the purification of molecules which otherwise would be very difficult to separate due to their similar physicochemical properties.

While most of the known metallosupramolecular structures are Werner-type coordination complexes, in the last five years a number of organometallic supramolecular architectures have emerged, most of them based on the use of N-heterocyclic carbenes (NHCs).[8] However, due to the scarcity of ligands of the appropriate sizes, most known organometallic metallosupramolecules are too small to host organic molecules, and this explains why organometallic host-guest chemistry is rare. Advancing organometallic host-guest chemistry is possible through the development of poly-NHC ligands that mimic the supramolecular architectures facilitated by Werner-type ligands, thus allowing the preparation of arguably more stable organometallic assemblies supported by the strong NHC-M bonds. By designing a series of NHC ligands decorated with rigid polyaromatic functionalities,[9] we recently gained access to a number of organometallic supramolecular complexes, which we used for the recognition of different organic molecules[6f, 7i, 10] and metal cations.[11] In one of our approaches, we formed two nickel-cornered molecular rectangles using a pyrene-bis-imidazolylidene ligand (**B** and **C**, Scheme 1).[7i] The two-dimensional complexes **B** and **C** resemble the previously reported molecular rectangle **A**, described by Hahn and co-workers in 2008.[12] However, while **A** was unsuitable even for the recognition of the smaller PAHs due to the relatively short separation provided by the benzoimidazolylidene ligand (10.4 Å), **B** and **C** served as effective receptors and scavengers of a range of polyaromatic molecules, due to the longer separation provided by the pyrene-bisimidazolylidene ligand (13 Å), and due to the effective steric and electronic complementarity. We recently became interested in obtaining a three-dimensional molecular cage based on the same organometallic supramolecular motif as the one used in **B** and **C**. We envisaged that, if **B** and **C** were able to effectively encapsulate two-dimensional organic molecules by multiple synergistic aromatic interactions, a related three-dimensional cage should be able to recognize 3-D organic molecules, such as fullerenes. Additionally, we hypothesized that a relatively rigid organometallic supramolecular cage should render size-dependent selective complexation of fullerenes. Finding systems for the selective encapsulation of fullerenes,[6b] and especially finding receptors for the selective complexation of C_{70} over C_{60}, is a challenging field of research that continuous to gain interest. In this communication, we describe the preparation of a three-dimensional nickel-cornered trigonal prism constituted by pyrene-di-imidazolylidene and 1,3,5-tripyridyl-triazine (TPT) ligands. This cage shows highly selective complexation of C_{70} over C_{60}.
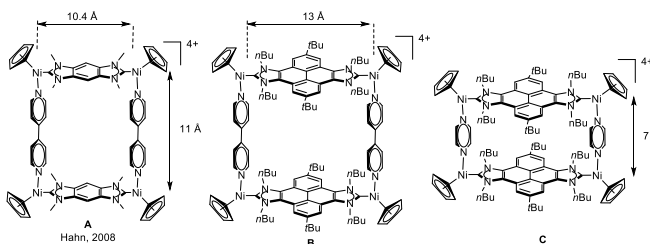

Scheme 1. Nickel-conjoined molecular rectangles

[a] Víctor Martínez-Agramunt and Prof. Eduardo Peris
Institute of Advanced Materials (INAM). Universitat Jaume I. Av. Vicente Sos Baynat s/n. Castellón. E-1271. Spain. Email: eperis@uji.es
[b] Prof. D. G. Gusev
Dept. of Chemistry and Biochemistry, Wilfrid Laurier University, Waterloo, Ontario N2L 3C5 (Canada). Email: dgoussev@wlu.ca

Supporting information for this article is given via a link at the end of the document.((Please delete this text if not appropriate))

Results and discussion

The reaction of the bis-nickel-pyrene-di-imidazolylidene complex **1** with TPT and two equivalents of AgBF$_4$ in dichloromethane afforded the air-stable metallocage **2** as a red solid, in 60% yield after purification (Scheme 2). The hexametallic complex **2** was characterized by NMR spectroscopy, mass spectrometry and elemental analysis. The correct stoichiometry of the cage was confirmed by ESI-TOF-MS, which showed peaks at m/z 1161.2 and 1785.2 assigned to [**2**-3BF$_4$]$^{3+}$ and [**2**-2BF$_4$]$^{4+}$, respectively. The formation of a single assembly was further confirmed by Diffusion-ordered NMR spectroscopy (DOSY), which revealed that all the proton signals showed the same diffusion coefficient in deuterated acetone 2.7×10^{-10} m^{2}s^{-1} (see SI for details). By using the Stokes-Einstein equation, this coefficient provides an estimated hydrodynamic radius of 6.2 Å, in a good agreement with the expected radius of **2** based on the known size of the bis-NHC and TPT ligands.
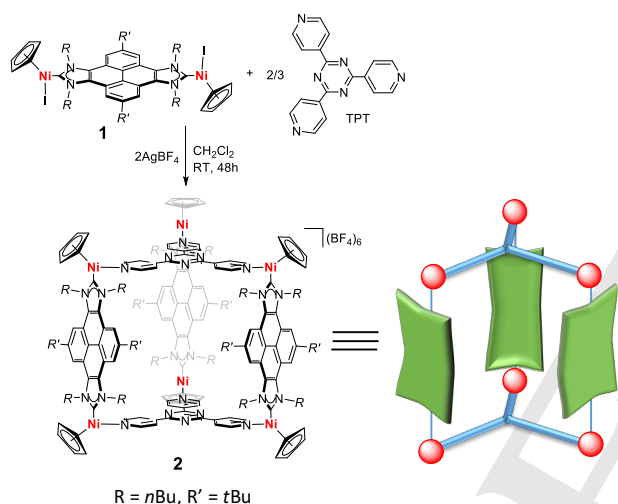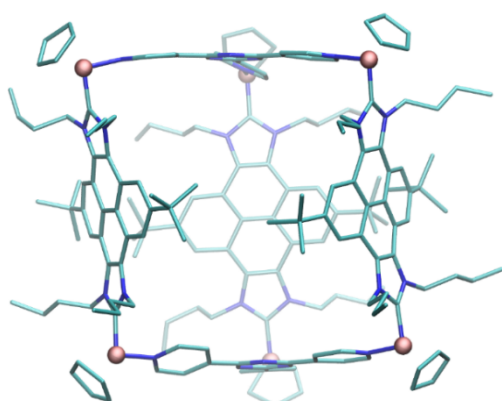

Scheme 2. Synthesis of metallocage **2**

Figure 1. X-Ray molecular structure of **2**. The counter-anions (6BF$_4^-$) and solvent (dichloroethane) are omitted for clarity.

The molecular structure of **2** was determined by X-ray diffraction (Figure 1). The molecule contains six nickel atoms connected by two TPT ligands and three pyrene-di-imidazolylidenes, thus forming a trigonal prism with pseudo-D_{3h} symmetry. The central pyrene fragments of the bis-NHC ligands are bent along the corresponding Ni-Ni axis, resulting in a convex curvature with respect to the inner cavity of the cage. The same pyrene fragments also show a concave curvature along the axis defined by the corresponding *tert*-butyl groups. These two distortions make the trigonal prism look as if tied around by an imaginary belt, as reflected by the average distance between the centroid of the cage and the two central carbons of the pyrenes (6.89 Å), and the average distance between the centroid of the TPT ligand and the nickel atoms (7.43 Å). The average Ni-Ni through-space distance across the bis-NHC ligand is 12.93 Å, that is practically the same as the average Ni-Ni distance along the triangular face of the prism, 12.86 Å. The effective size of the central cavity[13] is 1028 Å^3.

Considering the size of the internal cavity of **2** and the polyaromatic nature of its surface, we envisioned that this molecule might be a good system for studying supramolecular binding of fullerenes. We first performed an experiment that involved dissolving **2** in acetone-d_6 in the presence of a suspension of C$_{60}$ in an NMR tube. The product mixture was sonicated at room temperature, and changes in the sample were followed by ^{1}H NMR spectroscopy. In this experiment we took advantage of the high solubility of **2** in acetone, the solvent where C$_{60}$ is practically insoluble, so that the fullerene could become NMR-observable only if captured by the metallocage.

As can be seen from the spectra presented in Figure 2, we initially observed the ^{1}H NMR spectrum of the empty molecular cage **2**. After 1 h, a new species appeared in the spectrum, attributed to the formation of a host-guest complex C$_{60}$@**2**. The signal due to the protons of the pyrene-connecting group of the di-NHC ligand is upfield shifted with respect to the related signal of the empty cage. In addition, the signals due to the protons of the TPT ligand are downfield shifted with respect to the corresponding resonances of **2**. These observations are consistent with the fullerene being accommodated inside the cavity of **2** and interacting via π-stacking with the internal polyaromatic surface of the cage. The spectrum recorded after 8 h of reaction showed only the signals due to the C$_{60}$@**2** adduct, therefore indicating that the conversion was complete. A similar experiment was carried out using C$_{70}$ and provided similar results, affording clear evidence of formation of a C$_{70}$@**2** complex (see ESI for details).
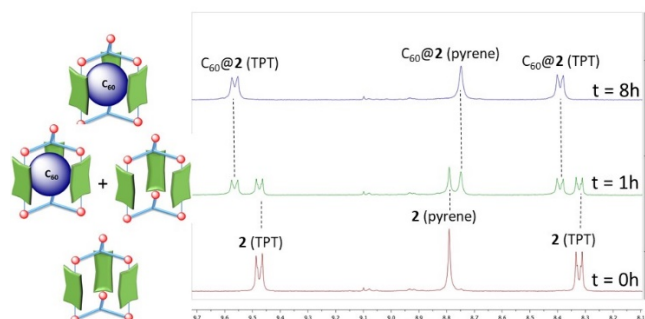

Figure 2. The aromatic region of ^{1}H NMR spectra of a mixture of **2** with C$_{60}$ in acetone-d_6. The spectra were recorded immediately after mixing, and 1 and 8 h later).

These experiments allowed us to isolate $C_{60}@\mathbf{2}$ and $C_{70}@\mathbf{2}$, by simply filtering off the remaining insoluble fullerenes, followed by solvent evaporation. The ^{13}C NMR spectra of the isolated $C_{60}@\mathbf{2}$ and $C_{70}@\mathbf{2}$ in acetone-d_6 displayed the characteristic signals due to the carbons of the fullerenes (see ESI for full details).

For the determination of the binding constants we found that a mixture of acetone/dichlorobenzene (1:4) provided the best solubilities for both the host and the guests. By using this solvent mixture, we observed that exchange of the free and bound host signals was slow on the NMR timescale, so integration of the distinct signals of free $\mathbf{2}$ and the complexes fullerene@$\mathbf{2}$ was used to calculate the equilibrium constants. This way, we obtained the binding constants of 4.7×10^3 and 3.5×10^4 M^{-1}, for the encapsulation of C_{60} and C_{70} at room temperature, respectively. This result indicates a preferred complexation of C_{70} over C_{60} of about one order of magnitude. The constants obtained are very large, especially considering that they were obtained using a mixture of solvents containing 80% dichlorobenzene, a good solvent for fullerenes for which lower association constants are often observed.[14]
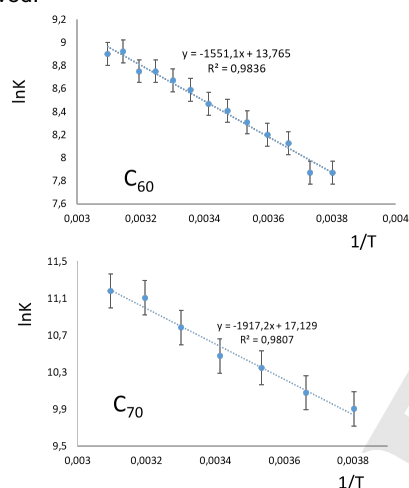

C[60] plot: $y = -1551.1x + 13.765$, $R^2 = 0.9836$
C[70] plot: $y = -1917.2x + 17.129$, $R^2 = 0.9807$

Figure 3. Plots of lnK *vs*. 1/T. The plots were built by using the binding constants obtained from the ^{1}H NMR spectra taken at different temperatures, from equimolar solutions (0.3 mM) of $\mathbf{2}$ and fullerene in acetone-d_6:dichlorobenzene-d_4 1:4. Error bands assume uncertainties of 10% (C_{60}) and 20% (C_{70}) in binding constant values.

By recording variable-temperature ^{1}H NMR spectra, we obtained a series of binding constants that allowed us to determine the association enthalpies and entropies from the related Van't Hoff plots (Figure 3). The thermodynamic values obtained for the association of C_{60} were $\Delta H = 3.1$ kcal/mol and $\Delta S = 27$ cal/molK. For C_{70}, the values were $\Delta H = 3.8$ kcal/mol and $\Delta S = 34$ cal/molK. It is worth noting that the thermodynamic values obtained for the C_{70} case are affected by a higher error than those obtained for the C_{60} case, due to the difficulties observed for the determination of the constants at the lower temperatures, because the overlapping of the signals forced us to estimate the constants by deconvolution. With these data in hand, we concluded that the low enthalpies and relatively large entropies observed indicate that the encapsulation of fullerenes by $\mathbf{2}$ is assisted by the intrinsic

entropic contribution (-TΔS), to afford negative free energy changes. Thus, the complexation is entropically favored by desolvation of the host and the guest. The complexation of C_{70} shows a greater value of ΔS due to the larger number of solvent molecules bound to C_{70} relative to C_{60}, as a consequence of the larger molecular surface of the former. The endothermicity of the associations is explained by the large solvation enthalpies of the host and guest. E.g., experimental solvation energies of -30.5 and -35.3 kcal/mol were reported for C_{60} and C_{70} respectively, in *o*-dichlorobenzene.[15]

Given the greater effective affinity of the metallocage $\mathbf{2}$ for C_{70} over C_{60}, we designed two competitive experiments aiming to provide practical experimental procedures for the separation of these two types of fullerenes. In the first experiment (Figure 4a), we suspended an equimolar mixture of C_{60} and C_{70} in acetone-d_6, and added one equivalent of $\mathbf{2}$; then the mixture was sonicated for 6 h. The analysis of the solution by ^{13}C NMR and mass spectrometry, indicated that only C_{70} was trapped by $\mathbf{2}$. The suspension was filtered off, and the black solid was redissolved in dichlorobenzene-d_4. The ^{13}C NMR of this sample confirmed the presence of the remaining pure C_{60} in this solution. In the second experiment (Figure 4b), a suspension of C_{60} and an equivalent amount of $\mathbf{2}$ were sonicated in acetone-d_6 until quantitative encapsulation of the fullerene. The presence of C_{60} inside the cavity of $\mathbf{2}$ was confirmed by ^{13}C NMR spectroscopy and mass spectrometry. Then, one equivalent of C_{70} was added to the mixture, and the suspension was sonicated for 6 h. The analysis of the resulting solution indicated that C_{70} had replaced C_{60} in the interior of the cavity, while the analysis of the solid confirmed the release of C_{60}. These two simple experiments illustrate how the metallocage $\mathbf{2}$ can be used as a convenient molecular receptor for selective fullerene binding and release, and thus practical applications for the purification of fullerenes may be envisaged.
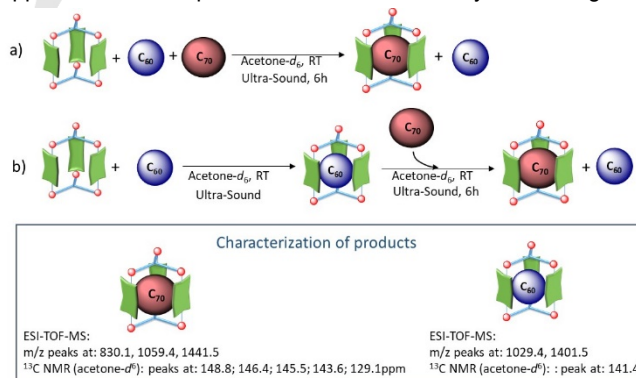

Characterization of products

ESI-TOF-MS:
m/z peaks at: 830.1, 1059.4, 1441.5
^{13}C NMR (acetone-d^6): peaks at: 148.8; 146.4; 145.5; 143.6; 129.1ppm

ESI-TOF-MS:
m/z peaks at: 1029.4, 1401.5
^{13}C NMR (acetone-d^6): : peak at: 141.4

Figure 4. Schematic representation of competitive experiments, together with the characterization data of the resulting host:guest complexes formed.
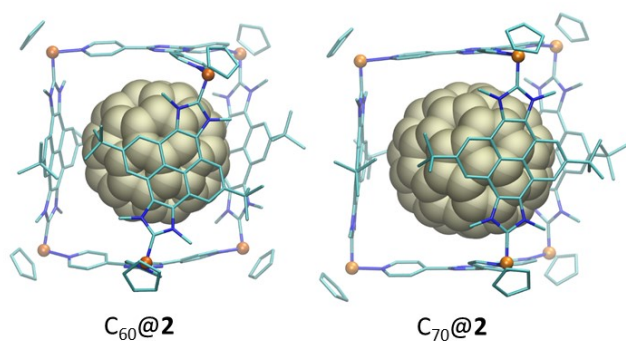
Figure 5. DFT-optimized structures of $C_{60}@2$ (left) and $C_{70}@2$ (right).

We performed DFT (M06-L/Def2SVP in *o*-dichlorobenzene solvent continuum) and semi-empirical (PM7) studies (see SI for details) to obtain more information about the geometries and binding energies of the complexes produced by the encapsulation of C_{60} and C_{70} in **2** (Figure 5). According to the DFT calculations, the cage of $C_{70}@2$ retains the approximate D_{3h} symmetric shape of **2**, and the hexametallic prism of the calculated structure does not reveal significant structural distortions compared to the experimental structure of Figure 1. These observations are also confirmed by the effective volume of the cage of $C_{70}@2$ (880 Å^3), which is slightly smaller compared to that in the empty **2** (*vide supra*).

The optimized geometry of $C_{60}@2$ reveals how the hexanickel molecular prism can adapt its shape to wrap around the smaller molecule of C_{60} by twisting the structure about the *z* axis, thus yielding a molecular shape of the pseudo D_{3d} symmetry. This deformation of the cage closes the distance between the top and bottom TPT ligands and allows a tighter interaction between the surface of the fullerene and the polyaromatic walls of the cage. The twisting of the cage results in a very significant shrinkage of the effective volume, from 1028 Å^3 in **2** to 698 Å^3 in $C_{60}@2$.[16]

The computational study provided data allowing to calculate the enthalpy and Gibbs energy of the substitution reaction: $C_{60}@2$ + $C_{70} \rightarrow C_{70}@2 + C_{60}$, ΔH = -3.8 and ΔG = -6.0 kcal/mol at 298 K, in *o*-dichlorobenzene. The calculated substitution entropy, ΔS = 7.5 cal·mol^{-1}·K^{-1} is the same as the difference between the experimental encapsulation entropies of C_{60} and C_{70}, ΔS = 7 cal·mol^{-1}·K^{-1}, although the excellent agreement is probably fortuitous. We note, however, that the calculated encapsulation enthalpy of C_{70} suggests a more favorable process than that of C_{60}, whereas the experimental encapsulation enthalpies are practically the same for both fullerenes. The ΔH values are relatively small; thus, they can be influenced by both computational and experimental errors. Nevertheless, proposing that the larger C_{70} can be more favorably accommodated in **2** *vs*. the smaller C_{60} is not unreasonable.

Conclusions

In summary, we prepared a NHC-based molecular prism that acts as a selective receptor for C_{70} over C_{60}, and facilitates the selective binding of the former from a mixture of the two. We also proved that the cage shows fullerene binding and release properties, with potential applications in the purification of mixtures of fullerenes. The supramolecular cage is able to modulate the size of the cavity for adapting to the shape of the fullerene host, thus it can be considered as a 'breathable' structure. Our work also demonstrates how NHC ligands can provide a competitive alternative to the classical Werner-type ligands in the design of supramolecular coordination cages for host-guest chemistry purposes.

[1] a) C. J. Brown, F. D. Toste, R. G. Bergman, K. N. Raymond, *Chem. Rev.* **2015**, *115*, 3012-3035; b) S. H. A. M. Leenders, R. Gramage-Doria, B. de Bruin, J. N. H. Reek, *Chem. Soc. Rev.* **2015**, *44*, 433-448; c) P. Dydio, J. N. H. Reek, *Chem. Sci.* **2014**, *5*, 2135-2145; d) T. S. Koblenz, J. Wassenaar, J. N. H. Reek, *Chem. Soc. Rev.* **2008**, *37*, 247-262; e) M. Raynal, P. Ballester, A. Vidal-Ferran, P. W. N. M. van Leeuwen, *Chem. Soc. Rev.* **2014**, *43*, 1660-1733; f) I. Sinha, P. S. Mukherjee, *Inorg. Chem.* **2018**, DOI: 10.1021/acs.inorgchem.1027b03067.

[2] a) S. Dong, B. Zheng, F. Wang, F. Huang, *Acc. Chem. Res.* **2014**, *47*, 1982-1994; b) K. Ariga, H. Ito, J. P. Hill, H. Tsukube, *Chem. Soc. Rev.* **2012**, *41*, 5800-5835; c) B. Chen, S. Xiang, G. Qian, *Acc. Chem. Res.* **2010**, *43*, 1115-1124.

[3] A. Galan, P. Ballester, *Chem. Soc. Rev.* **2016**, *45*, 1720-1737.

[4] a) A. Schmidt, V. Molano, M. Hollering, A. Poethig, A. Casini, F. E. Kuehn, *Chem. Eur. J.* **2016**, *22*, 2253-2256; b) Y.-R. Zheng, K. Suntharalingam, T. C. Johnstone, S. J. Lippard, *Chem. Sci.* **2015**, *6*, 1189-1193; c) B. Therrien, in *Chemistry of Nanocontainers, Vol. 319* (Eds.: M. Albrecht, F. E. Hahn), **2012**, pp. 35-55; d) F. Schmitt, J. Freudenreich, N. P. E. Barry, L. Juillerat-Jeanneret, G. Suess-Fink, B. Therrien, *J. Am. Chem. Soc.* **2012**, *134*, 754-757; e) N. P. E. Barry, O. Zava, P. J. Dyson, B. Therrien, *Chem. Eur. J.* **2011**, *17*, 9669-9677; f) O. Zava, J. Mattsson, B. Therrien, P. J. Dyson, *Chem. Eur. J.* **2010**, *16*, 1428-1431; g) B. Therrien, G. Suess-Fink, P. Govindaswamy, A. K. Renfrew, P. J. Dyson, *Angew. Chem. Int. Ed.* **2008**, *47*, 3773-3776; h) T. R. Cook, V. Vajpayee, M. H. Lee, P. J. Stang, K.-W. Chi, *Acc. Chem. Res.* **2013**, *46*, 2464-2474.

[5] a) A. M. Castilla, W. J. Ramsay, J. R. Nitschke, *Acc. Chem. Res.* **2014**, *47*, 2063-2073; b) G. H. Clever, P. Punt, *Acc. Chem. Res.* **2017**, *50*, 2233-2243; c) M. Han, D. M. Engelhard, G. H. Clever, *Chem. Soc. Rev.* **2014**, *43*, 1848-1860; d) C. Lescop, *Acc. Chem. Res.* **2017**, *50*, 885-894; e) S. Zarra, D. M. Wood, D. A. Roberts, J. R. Nitschke, *Chem. Soc. Rev.* **2015**, *44*, 419-432.

[6] a) T. K. Ronson, W. Meng, J. R. Nitschke, *J. Am. Chem. Soc.* **2017**, *139*, 9698-9707; b) C. Garcia-Simon, M. Costas, X. Ribas, *Chem. Soc. Rev.* **2016**, *45*, 40-62; c) N. Kishi, M. Akita, M. Yoshizawa, *Angew. Chem. Int. Ed.* **2014**, *53*, 3604-3607; d) C. Garcia-Simon, M. Garcia-Borras, L. Gomez, T. Parella, S. Osuna, J. Juanhuix, I. Imaz, D. Maspoch, M. Costas, X. Ribas, *Nat. Commun.* **2014**, *5*; e) P. D. Frischmann, S. H. M. Mehr, B. O. Patrick,

F. Lelj, M. J. MacLachlan, *Inorg. Chem.* **2012**, *51*, 3443-3453; f) C. Mejuto, L. Escobar, G. Guisado-Barrios, P. Ballester, D. Gusev, E. Peris, *Chem. Eur. J.* **2017**, *23*, 10644-10651; g) A. Sygula, *Synlett* **2016**, *27*, 2070-2080; h) T. Kawase, H. Kurata, *Chem. Rev.* **2006**, *106*, 5250-5273; i) D. Canevet, E. M. Perez, N. Martin, *Angew. Chem. Int. Ed.* **2011**, *50*, 9248-9259.

[7] a) R. Govindarajan, R. Nagarajaprakash, B. Manimaran, *Inorg. Chem.* **2015**, *54*, 10686-10694; b) E. M. Lopez-Vidal, A. Fernandez-Mato, M. D. Garcia, M. Perez-Lorenzo, C. Peinador, J. M. Quintela, *J. Org. Chem.* **2014**, *79*, 1265-1270; c) C. Alvarino, E. Pia, M. D. Garcia, V. Blanco, A. Fernandez, C. Peinador, J. M. Quintela, *Chem. Eur. J.* **2013**, *19*, 15329-15335; d) V. Blanco, M. D. Garcia, A. Terenzi, E. Pia, A. Fernandez-Mato, C. Peinador, J. M. Quintela, *Chem. Eur. J.* **2010**, *16*, 12373-12380; e) C. Peinador, E. Pia, V. Blanco, M. D. Garcia, J. M. Quintela, *Org. Lett.* **2010**, *12*, 1380-1383; f) M. H. Yuan, F. Weisser, B. Sarkar, A. Garci, P. Braunstein, L. Routaboul, B. Therrien, *Organometallics* **2014**, *33*, 5043-5045; g) M. D. Garcia, C. Alvarino, E. M. Lopez-Vidal, T. Rama, C. Peinador, J. M. Quintela, *Inorg. Chim. Acta* **2014**, *417*, 27-37; h) N. Kishi, Z. Li, Y. Sei, M. Akita, K. Yoza, J. S. Siegel, M. Yoshizawa, *Chem. Eur. J.* **2013**, *19*, 6313-6320; i) V. Martinez-Agramunt, S. Ruiz-Botella, E. Peris, *Chem. Eur. J.* **2017**, *23*, 6675-6681.

[8] N. Sinha, F. E. Hahn, *Acc. Chem. Res.* **2017**, *50*, 2167-2184.

[9] a) E. Mas-Marza, J. A. Mata, E. Peris, *Angew. Chem. Int. Ed.* **2007**, *46*, 3729-3731; b) S. Gonell, M. Poyatos, E. Peris, *Chem. Eur. J.* **2014**, *20*, 9716-9724; c) A. Prades, E. Peris, M. Alcarazo, *Organometallics* **2012**, *31*, 4623-4626; d) H. Valdes, M. Poyatos, E. Peris, *Organometallics* **2015**, *34*, 1725-1729; e) H. Valdes, M. Poyatos, E. Peris, *Organometallics* **2014**, *33*, 394-401; f) S. Ibañez, M. Poyatos, E. Peris, *Chem. Commun.* **2017**, *53*, 3733-3736.

[10] a) D. Nuevo, S. Gonell, M. Poyatos, E. Peris, *Chem. Eur. J.* **2017**, *23*, 7272-7277; b) C. Biz, S. Ibañez, M. Poyatos, D. Gusev, E. Peris, *Chem. Eur. J.* **2017**, *23*, 14439-14444.

[11] S. Ibañez, M. Poyatos, E. Peris, *Angew. Chem. Int. Ed.* **2017**, *56*, 9786-9790.

[12] F. E. Hahn, C. Radloff, T. Pape, A. Hepp, *Organometallics* **2008**, *27*, 6408-6410.

[13] Estimation of volume was made using the swisspdb software, available at http://www.expasy.org/spdbv/.

[14] V. H. Le, M. Yanney, M. McGuire, A. Sygula, E. A. Lewis, *J. Phys. Chem. B* **2014**, *118*, 11956-11964.

[15] E. B. Stukalin, M. V. Korobov, N. V. Avramenko, *J. Phys. Chem. B* **2003**, *107*, 9692-9700.

[16] N. Guex, M. C. Peitsch, *Electrophoresis* **1997**, *18*, 2714-2723.

Entry for the Table of Contents

COMMUNICATION

A nickel-conjoined organometallic prism cage shows highly selective complexation of C_{70} over C_{60}. The supramolecular cage is able to modulate the size of the cavity for adapting to the shape of the fullerene host.
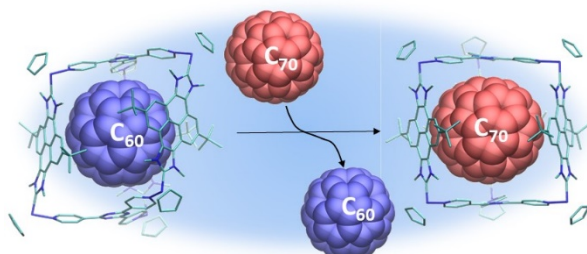
Víctor Martínez-Agramunt, Dmitry G. Gusev[and Eduardo Peris*

Page No. – Page No.

A shape-adaptable organometallic supramolecular coordination cage for the encapsulation of fullerenes